J. Am. Chem. Soc. **1983**, *105*, 396–402

Ab Initio Study of the Structures and Vibrational Spectra of the Hückel 4*n* Heterocycles Azirene, Oxirene, and Thiirene

P. Čársky,*† B. Andes Hess, Jr.,* and L. J. Schaad*

Contribution from the Department of Chemistry, Vanderbilt University, Nashville, Tennessee 37235. *Received April 26, 1982*

Abstract: Optimum geometries of thiirene, oxirene, and azirene were determined theoretically in ab initio SCF calculations using 3-21G and 4-31G basis functions. Vibrational frequencies and IR intensities were calculated for the three molecules and several isotopic derivatives. The theoretical thiirene vibrational spectra generally agree with the experimental but suggest that the C–S stretching frequency may be misassigned.

Introduction

The characterization of small antiaromatic ring systems[1] has provided a challenge to both the synthetic and theoretical chemist. Perhaps the best example of this is cyclobutadiene. Although initially thought to be a square structure,[2,3] theoretical calculations indicated it should be rectangular.[4–6] This disagreement was resolved when Masamune obtained a much improved IR spectrum[7] which is in good agreement with the calculated spectrum[8–10] of rectangular cyclobutadiene.

We describe here calculations on the structure and vibrational spectra of three related molecules, thiirene (**1**), oxirene (**2**) and azirene (**3**), not only to gain a better understanding of the structures of these three unusual systems but also to aid in the eventual identification of the as yet unknown **2** and **3**. Thiirene has been observed at low temperature[11,12] and its reported IR spectrum is in reasonable agreement with our earlier calculated spectrum.[13] We report here additional details of its calculated spectrum.

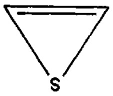
1

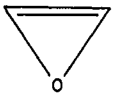
2

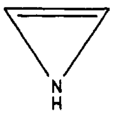
3

Equilibrium Geometries

All equilibrium geometries were obtained by using a modified version[14] of HONDO 5[15–18] in which the BMAT link of Pulay's program TEXAS[19–21] is incorporated so that optimization is carried out in internal coordinates rather than in atomic Cartesian coordinates, and an estimated second derivative matrix (used in the geometry optimization) is read in rather than using the standard form of the original HONDO. The internal coordinates used are shown in Figure 1. For oxirene and thiirene C_{2v} symmetry was assumed and for azirene C_s symmetry (though as shown in the Appendix the positive definite character of the computed force constant matrices implies that removing these symmetry restrictions will not lower the molecular energies). Earlier calculations on thiirene[13] and oxirene[22] were done with Pople and Hehre's 4-31G basis.[23] We have reoptimized the geometry of these two molecules using the new more economical 3-21G basis[24,25] designed particularly for geometry and force-constant calculations. Azirene was optimized in both basis sets. In Table I are listed the equilibrium geometries for **1–3** and in Table II their energies. Note that all three molecules have relatively long carbon–heteroatom bonds, which is indicative of their antiaromaticity. A similar situation exists with the unusually long C–C single bonds calculated for cyclobutadiene.[4–6,8,9] Furthermore, in the case of azirene the N–H bond is considerably out of plane, again indicating a driving force to minimize the conjugation of the unshared pair of electrons on nitrogen with the double bond. Clark had obtained a similar result for azirene in an earlier ab initio partial geometry optimization of azirene.[26] In addition we

Table I. Calculated Optimum Geometries[a]

bond length or angle	oxirene		thiirene		azirene	
	3-21G	4-31G[b]	3-21G	4-31G[c]	3-21G	4-31G
C–X	1.557	1.552	1.993	1.978	1.559	1.529
C=C	1.249	1.248	1.247	1.251	1.264	1.263
C- H	1.055	1.054	1.055	1.056	1.057	1.056
N–H					1.018	1.009
∠HCC	161.5	162.3	155.1	154.9	155.6	155.8
N–H bond out-of-plane angle					59.0	56.2
C–H bond out-of-plane angle					4.5[d]	4.3[d]

[a] Bond angles are in angstroms and angles in degrees. [b] Reference 22. [c] Reference 13. [d] The hydrogens on carbon are trans to the hydrogen on nitrogen.

Table II. Energies (au) of Oxirene, Thiirene, and Azirene

compound	3-21G	4-31G
oxirene	−150.728612	−151.35397[a]
thiirene	−471.915088	−473.725975[b]
azirene	−131.017494	−131.559809

[a] Reference 22. [b] Reference 13.

Table III. Symmetry Coordinates[a]

species	coordinates for oxirene and thiirene	species	coordinates for azirene
A_1	$S_1 = 2^{-1/2}(d_1 + d_2)$ $S_2 = d_3$ $S_3 = 2^{-1/2}(r_1 + r_2)$ $S_4 = 2^{-1/2}(\theta_1 + \theta_2)$	A'	$S_1 = 2^{-1/2}(d_1 + d_2)$ $S_2 = d_3$ $S_3 = 2^{-1/2}(r_1 + r_2)$ $S_4 = r_3$ $S_5 = 2^{-1/2}(\theta_1 + \theta_2)$ $S_6 = 2^{-1/2}(\beta_1 + \beta_2)$ $S_7 = 2^{-1/2}(\gamma_1 + \gamma_2)$
B_2	$S_5 = 2^{-1/2}(d_1 - d_2)$ $S_6 = 2^{-1/2}(r_1 - r_2)$ $S_7 = 2^{-1/2}(\theta_1 - \theta_2)$		
		A"	$S_8 = 2^{-1/2}(d_1 - d_2)$ $S_9 = 2^{-1/2}(r_1 - r_2)$ $S_{10} = 2^{-1/2}(\theta_1 - \theta_2)$ $S_{11} = 2^{-1/2}(\beta_1 - \beta_2)$ $S_{12} = 2^{-1/2}(\gamma_1 - \gamma_2)$
A_2	$S_8 = 2^{-1/2}(\gamma_1 - \gamma_2)$		
B_1	$S_9 = 2^{-1/2}(\gamma_1 + \gamma_2)$		

[a] See Figure 1 for definition of internal coordinates.

---

† J. Heyrovský Institute of Physical Chemistry and Electrochemistry, Czechoslovak Academy of Sciences, Prague, Czechoslovakia.

(1) Breslow, R. *Acc. Chem. Res.*, **1973**, *6*, 393.

(2) Chapman, O. L.; McIntosh, C. L.; Pacansky, J. *J. Am. Chem. Soc.* **1973**, *95*, 614.

(3) Krantz, A.; Lin, C. Y.; Newton, M. D. *J. Am. Chem. Soc.* **1973**, *95*, 2744.

(4) Kollmar, H.; Staemmler, V. *J. Am. Chem. Soc.* **1977**, *99*, 3583.

(5) Borden; W. T.; Davidson, E. R.; Hart, P. *J. Am. Chem. Soc.* **1978**, *100*, 388.

0002-7863/83/1505-0396$01.50/0

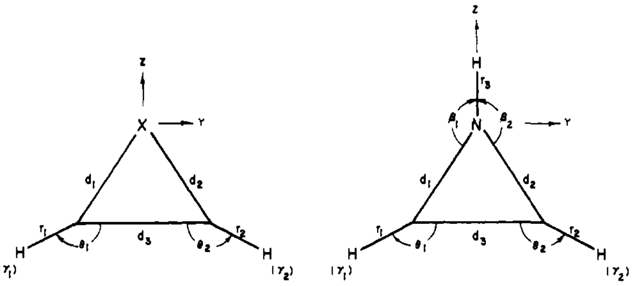

Figure 1. Structures of oxirene (X = O, C_{2v}), thiirene (X = S, C_{2v}), and azirene (C_s) and definition of internal coordinates. γ_1 and γ_2 are the out-of-plane bending angles.

Table IV. Calculated 3-21G Quadratic Force Constants[a] for Oxirene and Thiirene

constant	oxirene	thiirene
A_1 F_{11}	2.894	1.367
F_{22}	14.470	14.030
F_{33}	6.881	6.924
F_{44}	0.669	0.564
F_{12}	0.339	0.691
F_{13}	0.025	0.010
F_{14}	−0.104	−0.359
F_{23}	−0.201	−0.202
F_{24}	0.050	0.394
F_{34}	0.053	0.062
B_2 F_{55}	2.562	2.539
F_{66}	6.861	6.901
F_{77}	0.580	0.524
F_{56}	0.127	0.076
F_{57}	−0.751	−0.817
F_{67}	0.042	0.030
A_2 F_{88}	0.352	0.399
A_1 F_{99}	0.366	0.415

[a] Stretching force constants are in mdyne $Å^{-1}$, bending and wagging force constants in mdyne Å rad^{-2}, and stretching-bending interaction constants in mdyne rad^{-1}.

Table V. Calculated 3-21G Quadratic Force Constants for Azirene[a]

A' symmetry				A'' symmetry	
F_{11}	3.183	F_{24}	0.029	F_{88}	3.217
F_{22}	13.628	F_{25}	0.030	F_{99}	6.770
F_{33}	6.790	F_{26}	−0.150	$F_{10,10}$	0.635
F_{44}	6.786	F_{27}	0.068	$F_{11,11}$	2.304
F_{55}	0.732	F_{34}	0.008	$F_{12,12}$	0.433
F_{66}	0.732	F_{35}	0.059	F_{89}	0.142
F_{77}	0.377	F_{36}	−0.008	$F_{8,10}$	0.651
F_{12}	−0.060	F_{37}	0.001	$F_{8,11}$	−0.521
F_{13}	−0.019	F_{45}	−0.012	$F_{8,12}$	−0.128
F_{14}	−0.071	F_{46}	0.045	$F_{9,10}$	−0.061
F_{15}	−0.019	F_{47}	−0.048	$F_{9,11}$	−0.020
F_{16}	0.505	F_{56}	0.012	$F_{9,12}$	0.009
F_{17}	−0.058	F_{57}	−0.129	$F_{10,11}$	−0.116
F_{23}	−0.132	F_{67}	−0.007	$F_{10,12}$	−0.097
				$F_{11,12}$	−0.101

[a] See Table IV for units.

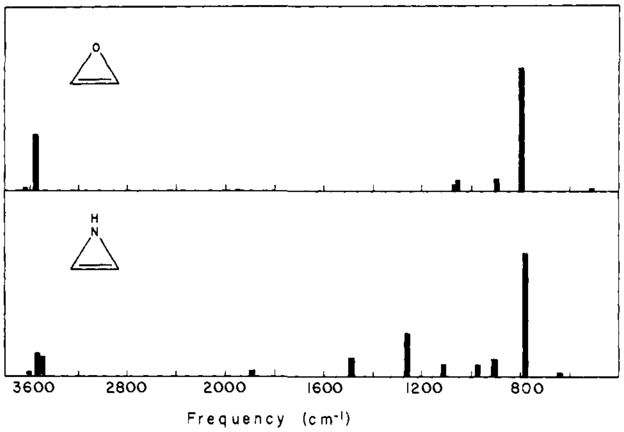

Figure 2. Computed IR spectra of oxirene and azirene in the 3-21G basis. Intensities are plotted relative to that of the strongest band.

find that the hydrogens on carbon are also out of the plane of the ring, being trans to the hydrogen on nitrogen. A comparison of the two basis sets results for all three molecules shows good agreement between them for both bond lengths and angles.

Force Constants, Vibrational Frequencies, and IR Intensities

Optimum 3-21G geometries of oxirene, thiirene, and azirene were adopted as reference geometries. Generally it is considered preferable to use experimental geometries[27] or empirically corrected theoretical geometries,[28] but with oxirene and azirene the molecules are not yet known and hence any attempt at an empirical correction would be uncertain. Starting with the reference geometry, each symmetry adapted internal coordinate in Table III was distorted, one by one, by $+\Delta S_i$ and then by $-\Delta S_i$. These displacements were chosen to make bond-length distortions equal ±0.05 au and bond angle changes ±3°. The changes in internal coordinates were transformed to atomic Cartesian coordinates by BMAT and read into HONDO, which computed the dipole moment and analytical gradient at each distortion. The gradient was transformed back to symmetrized internal coordinates by BMAT. The total number of gradient calculations was 14 for oxirene and thiirene (reference structure + eight distorted structures for A_1 coordinates and five structures for B_2, A_2, and B_1 coordinates) and 20 for azirene. These energy gradient and dipole moment results were read into a short program MAKEF which used them in a numerical computation of the force constant matrix and dipole moment gradient in internal coordinates. Averages of the values for $+\Delta S_i$ and $-\Delta S_i$ were used in this, and the positive and negative distortions also permitted[29] the evaluation of all diagonal and semidiagonal cubic force constants.[30] The force constant and dipole moment gradient matrices were then used with the mo-

---

(6) Jafri, J. A.; Newton, M. D. *J. Am. Chem. Soc.* **1978**, *100*, 5012.

(7) Masamune, S.; Souto-Bachiller, F. A.; Machiguchi, T.; Bertie, J. E. *J. Am. Chem. Soc.* **1978**, *100*, 4889.

(8) Kollmar, H.; Staemmler, V. *J. Am. Chem. Soc.* **1978**, *100*, 4304.

(9) Schaad, L. J.; Hess, B. A., Jr.; Ewig, C. S. *J. Am. Chem. Soc.* **1979**, *101*, 2281.

(10) Schaad, L. J.; Hess, B. A., Jr.; Ewig, C. S. *J. Org. Chem.* **1982**, *47*, 2904.

(11) Krantz, A.; Laureni, J. *J. Am. Chem. Soc.* **1981**, *103*, 486.

(12) Torres, M.; Safarik, I.; Clément, A.; Bertie, J. E.; Strausz, O. P. *Nouv. J. Chim.* **1979**, *3*, 365.

(13) Hess, B. A., Jr.; Schaad, L. J.; Ewig, C. S. *J. Am. Chem. Soc.* **1980**, *102*, 2507.

(14) Hess, B. A., Jr.; Schaad, L. J.; Ewig, C. S., Čársky, P., *J. Comput. Chem.*, in press.

(15) King, J. F.; Dupuis, M. *J. Comput. Phys.* **1976**, *21*, 144.

(16) Dupuis, M.; Rys, J.; King, H. F. *J. Chem. Phys.* **1976**, *65*, 111.

(17) Dupuis, M.; King, H. F. *Int. J. Quantum Chem.* **1977**, *11*, 613.

(18) Dupuis, M.; King, H. F. *J. Chem. Phys.* **1978**, *68*, 3998.

(19) Pulay, P. *Theor. Chim. Acta* **1979**, *50*, 299.

(20) Pulay, P. *Mol. Phys.* **1969**, *17*, 197.

(21) Pulay, P. In "Modern Theoretical Chemistry"; Vol. 4; Schaefer, H. F., III, Ed.; Plenum Press: New York, 1977; pp 153–185.

(22) Tanaka, K.; Yoshimine, M. *J. Am. Chem. Soc.* **1980**, *102*, 7655.

(23) (a) Ditchfield, R.; Hehre, W. J.; Pople, J. A. *J. Chem. Phys.* **1971**, *54*, 724. (b) Hehre, W. J.; Lathan, W. A. *Ibid.* **1972**, *56*, 5255.

(24) Binkley, J. S.; Pople, J. A.; Hehre, W. J. *J. Am. Chem. Soc.* **1980**, *102*, 939.

(25) Gordon, M. S.; Binkley, J. S.; Pople, J. A.; Pietro, W. J.; Hehre, W. J. *J. Am. Chem. Soc.* **1982**, *104*, 2797.

(26) Clark, D. T. In "Quantum Aspects of Heterocyclic Compounds in Chemistry and Biochemistry"; Bergmann, E. D., Pullman, B., Eds.; Israel Academy of Sciences: Jerusalem, 1970; p 238.

(27) Schwendeman, R. H. *J. Chem. Phys.* **1966**, *44*, 2115.

(28) Blom, C. E.; Altona, C. *Mol. Phys.* **1976**, *31*, 1377.

(29) Pulay, P.; Forgarasi, G.; Pang, F.; Boggs, J. E. *J. Am. Chem. Soc.* **1979**, *101*, 2550.

(30) These are available from the authors on request.

Table VI. Vibrational Frequencies (cm^{-1}) of Thiirene and Its Symmetrically Substituted Isotopic Derivatives Calculated with the 3-21G Basis Set[a]

symmetry		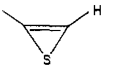	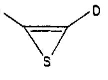	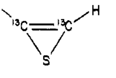
A_1	ring def (C-S str)[b]	478 (1095)	475 (1070)	467 (1047)
	C-H(D) bend, in-plane	937 (4)	675 (22)	937 (4)
	C=C stretch	1909 (605)	1753 (377)	1844 (570)
	C-H(D) stretch	3623 (799)	2805 (849)	3603 (749)
B_1	C-H(D) bend, out-of-plane	843 (6855)	630 (3489)	839 (6848)
B_2	ring def	424 (11)	410 (3)	410 (11)
	C-H(D) bend, in-plane	969 (2238)	741 (1156)	964 (2234)
	C-H(D) stretch	3547 (2828)	2605 (1640)	3537 (2790)
A_2	C-H(D) bend, out-of-plane	964	792	951

[a] IR intensities in km mol^{-1} are in parentheses. [b] These descriptions are of course approximate. In particular there is considerable mixing of the C-S stretch and the symmetric in-plane C-H(D) bend.

Table VII. Vibrational Frequencies (cm^{-1}) of Thiirene and Its Unsymmetrically Substituted Isotopic Derivatives Calculated with the 3-21G Basis Set[a]

sym-metry		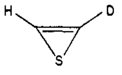	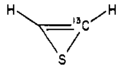
A'	ring def[b]	417 (6)	417 (19)
	ring def (C-S str)	476 (1084)	473 (1063)
	C-D(H) bend, in-plane	707 (427)	937 (4)
	C-H bend, in-plane	955 (1281)	967 (2236)
	C=C stretch	1824 (473)	1877 (588)
	C-D(H) stretch	2709 (1317)	3541 (2786)
	C-H stretch	3588 (1816)	3613 (797)
A''	C-D(H) bend, out-of-plane	690 (3444)	841 (6845)
	C-H bend, out-of-plane	925 (1727)	958 (6)

[a] IR intensities in km mol^{-1} are in parentheses. [b] See corresponding footnote to Table VI.

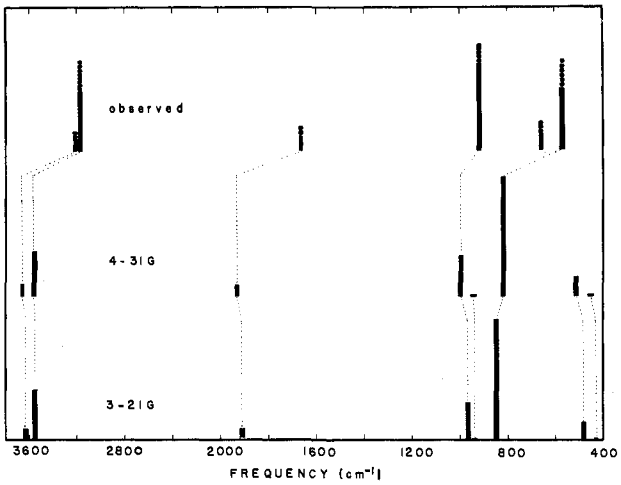

Figure 3. IR spectrum of thiirene. Intensities are relative to the strongest band. The observed frequencies and intensities are taken from ref 11, 12, and 33 (see text).

lecular geometry in a program GFMAT which did a standard Wilson GF analysis to give the vibrational frequencies and their normal modes. GFMAT also combines the normal mode eigenvectors with the dipole moment gradient to give the $\partial\mu/\partial Q_k$ which were then used to compute integrated infrared band intensities:

$$A_k = \frac{1}{cL}\int \log (I/I_0)\, d\nu \qquad (1)$$

where c is concentration in mol L^{-1} and L is the optical path in cm, and approximated by

$$A_k = \frac{N_A \pi}{3000c^2 \times 2.302581}|\partial\mu/\partial Q_k|^2 \qquad (2)$$

where N_A is Avogradro's number in mol^{-1}, c is the light velocity in cm s^{-1}, and $\partial\mu/\partial Q_k$ is the dipole moment derivative with respect to the kth normal coordinate Q_k. The derivatives $\partial\mu/\partial Q_k$ are expressed in D Å^{-1} u$^{-1/2}$, u being the unified atomic unit $M(^{12}C)/12 = 1.660565 \times 10^{-27}$ kg. The intensity A_k is therefore expressed by (2) in km mol^{-1}. With isotopic species the intensities were calculated from $\partial\mu_x/\partial S_i$, $\partial\mu_y/\partial S_i$ and $\partial\mu_z/\partial S_i$ for the parent systems by applying the rotational correction as described in ref 29. The calculated Raman and IR frequencies and IR intensities for compounds **1**-**3** and their isotopic derivatives are given in Tables VI-VIII. In Figure 2 are plotted the spectra of oxirene and azirene. In Figure 3 are plotted the calculated 3-21G and 4-31G spectra of thiirene. As was the case of the geometries discussed above, agreement is excellent both in the calculated frequencies and intensities between the two basis sets. In Figures 4-6 are plotted the spectra of the thiirene isotopic derivatives.

Comparison and Discussion of the Calculated and Experimental Spectra of Thiirene

Experimental IR spectra have been reported for thiirene and several of its isotopic derivatives by two groups.[11,12] The thiirenes were formed photochemically at 8 K in a frozen matrix and

Table VIII. Vibrational Frequencies (cm^{-1}) of Oxirene and Its Symmetrically Substituted Isotopic Derivatives Calculated with the 3-21G Basis Set[a]

symmetry		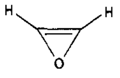	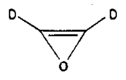	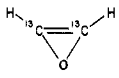
A_1	ring def (C-O str)[b]	885 (632)	924 (66)	875 (577)
	C-H(D) bend, in-plane	1051 (503)	727 (625)	1045 (558)
	C=C stretch	1944 (30)	1769 (10)	1879 (27)
	C-H(D) stretch	3620 (224)	2822 (185)	3598 (214)
B_1	C-H(D) bend, out-of-plane	793 (5906)	593 (2873)	789 (5922)
B_2	ring def	513 (181)	499 (104)	499 (173)
	C-H(D) bend, in-plane	1055 (351)	826 (308)	1047 (341)
	C-H(D) stretch	3536 (2754)	2596 (1450)	3525 (2741)
A_2	C-H(D) bend, out-of-plane	914	754	901

[a] IR intensities in km mol^{-1} are in parentheses. [b] See corresponding footnote to Table VI. C-O stretch and symmetric in plane C-H bend mix considerably and lead to the interchange of the first two A_1 levels in the dideuterio compound.

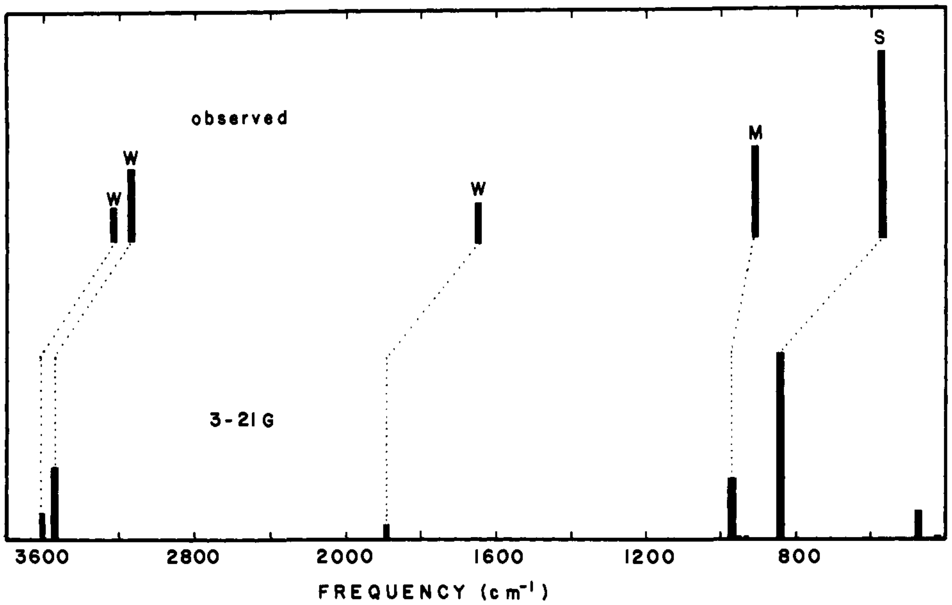

Figure 4. Computed and observed IR spectra of [2-^{13}C]thiirene. Intensities are relative to the strongest band. "Strong", "medium", and "weak" intensities in the experimental spectrum of ref 11 are arbitrarily represented here as relative intensities of 1.0, 0.5, and 0.2. The lower frequency C–H stretch is the sum of two weak lines superimposed.

Table IX. Vibrational Frequencies (cm^{-1}) of Oxirene and Its Unsymmetrically Substituted Isotopic Derivatives Calculated with the 3-21G Basis Set[a]

symmetry		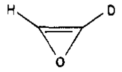	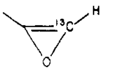
A'	ring def[b]	505 (134)	506 (177)
	ring def (C–O str)	912 (229)	880 (604)
	C–D(H) bend, in-plane	770 (521)	1046 (497)
	C–H bend, in-plane	1052 (552)	1053 (379)
	C=C stretch	1848 (40)	1912 (29)
	C–D(H) stretch	2714 (942)	3530 (2724)
	C–H stretch	3581 (1346)	3610 (242)
A''	C–D(H) bend, out-of-plane	651 (2957)	791 (5910)
	C–H bend, out-of-plane	876 (1431)	907 (4)

[a] IR intensities in km mol^{-1} are in parentheses. [b] See corresponding footnote to Table VI. Mixing of C–O stretch and C–D in-plane bend interchanges the second and third A' levels in the deuterio compound.

identified by their IR spectra in the reaction mixture. Their extreme reactivity precludes isolation and purification, and the presence of other products in the reaction mixture complicates the spectroscopy. Consequently although the two groups agree on most features of the spectra there are some differences. The published spectra[11,12,31,32] give only qualitative estimates (strong, medium, weak) of band intensities, but Professors Bertie and Torres[33] have kindly sent us quantitative relative band intensities for thiirene and its d_1 and d_2 derivatives with the caution that these must be considered rough estimates.

Experimental thiirene frequencies and relative intensities[11,33] are plotted at the top of Figure 3. Vertical heights are proportional to intensities with error estimates shown by the dotted extensions. Thus the minimum estimate of an intensity is shown by the solid line and the maximum by the solid plus dotted lines. Intensities were measured relative to the 910 cm^{-1} absorption; however, the line shown just above 900 cm^{-1} is the sum of this absorption and another at 912 cm^{-1}. These likely result from a single fundamental split by effects of the solid matrix. In any case the splitting is too small to appear on the scale of Figure 3. Similarly the more intense of the two lines of highest frequency is the sum of a pair at 3165 and 3169 cm^{-1}. Except for the band at 657 cm^{-1}, both experimental groups agree that all lines shown belong to thiirene. While Strausz, Bertie, and co-workers[12,31,32] assign the band at 657 cm^{-1} to the spectrum of thiirene, Krantz and Laureni[11] state that they are unable to conclude definitely that it does belong to thiirene. Although all calculated lines are displaced toward higher frequency, the theoretical patterns at the bottom of Figure 3 are in general agreement with observation except for the questionable absorption at 657 cm^{-1} and a disagreement on the relative intensities of the two strongest low-frequency lines. The two highest frequency lines are C–H stretches with the symmetric stretch being of higher frequency and lower intensity in the experimental and both theoretical spectra. The next lower frequency line is due to the C═C stretch. The most intense band in the theoretical spectrum is a B_1 C–H out-of-plane bend and corresponds to the experimental 563-cm^{-1} band. The other strong low-frequency band observed at 912 cm^{-1} is a C–H in-plane bend. Krantz[11] does not determine whether this is the A_1 or B_2 absorption. Strausz and Bertie[12] originally thought it to be the A_1, though Strausz,[31,32] now assigns it as B_2, in agreement with out theoretical result.

Strausz[12] assigns the questionable 657 cm^{-1} band to a symmetric ring deformation which must be largely due to a stretching of the C–S bonds. However, with the 3-21G basis this vibration is computed to lie much lower at 478 cm^{-1}. Since these SCF frequencies are too high, it seems most probable that the C–S stretch should not appear as high as 657 cm^{-1}. Some support for this is given by the fact that the analogous band in thiirane[34] is at 627 cm^{-1}. One might expect that the antiaromatic thiirene would have a weaker C–S bond than the saturated thiirane and therefore that the C–S stretch would lie at lower frequency than in thiirane. The long C—S bond, the very short C═C bond, and the large ∠HCC shown in Table I are all in accord with this and suggest the description of thiirene as a sulfur atom in fairly loose association with acetylene. Hence we predict that the symmetric C–S stretch in thiirene is yet to be observed somewhere below 400 cm^{-1}. It might be that the observed 657 cm^{-1} absorption corresponds to our very weak calculated symmetric in-plane C–H bend. This seems unlikely since the symmetric and antisymmetric combinations of C–H stretches and in-plane C–H bends are calculated to be separated by about the same amount, and the two C–H stretches are separated by much less in the observed spectrum

---

(31) Safarik, I.; Torres, M.; Strausz, O. P. *Chem. Phys. Lett.* **1980**, *72*, 388.

(32) Torres, M.; Lown, E. M.; Gunning, H. E.; Strausz, O. P. *Pure Appl. Chem.* **1980**, *52*, 1623.

(33) Bertie, J. E.; Torres, M., private communication.

(34) Bertie, J. E.; Othen, D. A.; Falk, M. V.; Mast, G. B., unpublished work.

Table X. Vibrational Frequencies (cm^{-1}) of Azirene and Its Isotopic Derivatives Calculated with the 3-21G Basis Set[a]

symmetry[b]	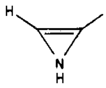	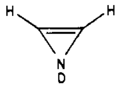	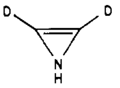	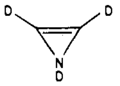	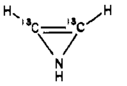	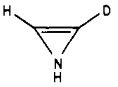	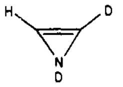	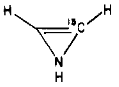
A'	775 (5639)	770 (5523)	585 (2969)	581 (2937)	772 (5614)	617 (318)	612 (513)	629 (233)
	906 (823)	904 (846)	736 (345)	735 (335)	899 (819)	646 (3286)	641 (3049)	773 (5625)
	1095 (42)	1065 (260)	968 (342)	961 (447)	1088 (47)	799 (334)	798 (327)	903 (821)
	1482 (976)	1134 (330)	1479 (966)	1107 (363)	1479 (994)	910 (1385)	878 (1819)	963 (542)
	1887 (299)	1887 (326)	1739 (173)	1738 (225)	1823 (268)	961 (743)	948 (693)	1090 (121)
	3502 (821)	2564 (488)	2770 (313)	2563 (452)	3502 (810)	1100 (293)	984 (341)	1103 (540)
	3583 (276)	3583 (231)	3502 (861)	2770 (337)	3564 (267)	1251 (1872)	1079 (349)	1250 (2018)
A''	638 (244)	635 (290)	604 (266)	599 (340)	622 (223)	1481 (969)	1127 (434)	1481 (985)
	969 (576)	908 (1258)	790 (583)	768 (790)	958 (503)	1807 (233)	1806 (271)	1856 (284)
	1107 (619)	1005 (9)	891 (279)	888 (320)	1095 (612)	2678 (494)	2563 (461)	3502 (811)
	1252 (1969)	1107 (700)	1250 (1782)	966 (310)	1248 (2068)	3502 (821)	2678 (512)	3506 (1020)
	3512 (1030)	3512 (1029)	2579 (590)	2579 (586)	3501 (1019)	3550 (638)	3550 (596)	3574 (280)

[a] IR intensities in km mol^{-1} are in parentheses. Internal coordinates mix extensively so that the normal modes are not in general simply describable. [b] The last three molecules have no symmetry.

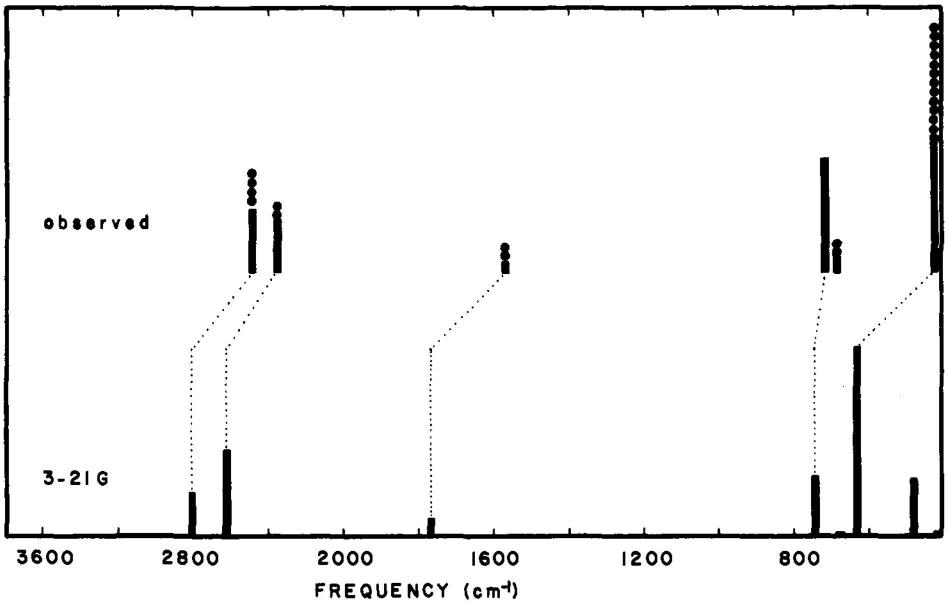

Figure 5. Computed and observed IR spectra of thiirene-d_2. Intensities are relative to the strongest band.

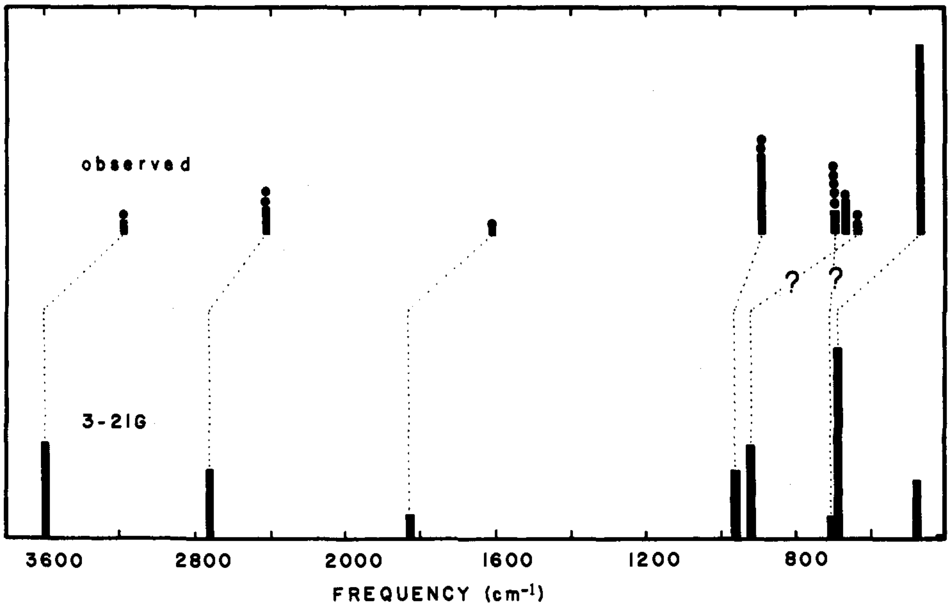

Figure 6. Computed and observed IR spectra of thiirene-d_1.

than is the 657 cm^{-1} line from the antisymmetric in-plane C–H bend. Experiment and theory differ on whether the B_1 C–H out-of-plane bend or the B_2 C–H in-plane bend is of greater intensity; we cannot predict which is correct. Like the A_1 in-plane C–H bend at 937 cm^{-1}, the B_2 ring deformation at 424 cm^{-1} is predicted to be too weak to be observed. The correlations indicated by dotted lines in Figures 3–6 are those we think most likely.

Further support for the above conclusions can be obtained by comparing the calculated and experimental spectra of the isotopic thiirenes. Figure 4 shows Krantz's reported spectrum of [2-^{13}C]thiirene.[11] The second line from the high-frequency end of the observed spectrum is the sum of two weak lines. Strausz and Bertie have not studied this compound, and quantitative estimates of intensities are not available, but there is good agreement between the qualitative intensities and those of the theoretical spectrum at the bottom of Figure 4. Krantz does not report any absorption in the vicinity of 657 cm^{-1}.

The experimental spectrum of thiirene-*d*$_2$ is shown in the upper half of Figure 5 with the 3-21G predictions below. Theoretical and observed patterns are quite similar. The antisymmetric C–D stretch is computed to be of somewhat higher intensity than the symmetric, whereas the opposite is true in the experimental spectrum. But the difference is probably within the error in both methods, and the frequency order is the same in the two. In both spectra the A_1 C=C stretch of weak intensity lies next followed by a stronger B_2 C—D in-plane bend. A weak absorption at 681 cm^{-1} is reported by Strausz[12] and assigned to the A_1 C–D in-plane bend. Krantz[11] does not report this line which does lie quite close to the predicted A_1 C–D in-plane bend at 675 cm^{-1}, but the predicted line would be expected to lie higher rather than lower than the observed. Further, the predicted intensity of this absorption is very low—only 0.006 times that of the strongest line. For these reasons the identification of the observed 681 cm^{-1} line with the A_1 C–D in-plane bend is not indicated in Figure 5. The strongest line in both spectra occurs next and is the B_1 C–D out-of-plane bend. No C–S stretch was observed, and again it is predicted to lie below the lowest reported absorption.

Calculated and experimental spectra of thiirene-*d*$_1$ are shown in Figure 6. The three bands of highest frequency are the C—H stretch, C—D stretch, and C=C stretch, in that order, though observed and calculated intensities are not in good agreement for C—H and C—D stretches. The next band in both spectra is the C–H in-plane bend with good agreement between observed and calculated intensities. The strongest absorption in both spectra is the C–D out-of-plane bend as shown. This leaves three lines in Strausz's spectrum between 600 and 700 cm^{-1}. None of the three are reported by Krantz, and the two shown by broken lines in Figure 6 are described as tentative by Strausz. The central line at 668 cm^{-1} is not tentative and is assigned by Strausz to the symmetric C–S stretch. Again we predict this should lie much lower. The C–H out-of-plane bend and the C–D in-plane bend in the theoretical spectrum are separated by much more than and are in opposite order from the two tentative absorptions in the observed spectrum that are given these assignments. However, in C_2H_2S the B_1 out-of-plane bend is computed to lie 280 cm^{-1} too high. Making this same correction to the computed C–H out-of-plane bend in C_2HDS gives (925 – 280) = 645 cm^{-1}, in good agreement with the observed 640 cm^{-1} band. Similarly a correction of 25 cm^{-1} from C_2D_2S for the C–D in-plane bend gives 682 cm^{-1} for C_2HDS, in good agreement with the observed 693 cm^{-1}. As a check, the C–H in-plane bend in C_2H_2S is computed to be 57 cm^{-1} too high, in good agreement with the 63 cm^{-1} error in C_2HDS; and the C–D out-of-plane bend in C_2D_2S is computed 211 cm^{-1} too high, in good agreement with the 222 cm^{-1} value in C_2HDS.

In summary, except for the C–S symmetric stretch which we suggest lies at much lower frequency than reported, quite good agreement between the calculated and observed spectra of thiirene has been found. In light of this it is hoped that the calculated spectra for the yet unknown oxirene and azirene will be useful in their eventual characterization.

Acknowledgment. We express our appreciation to the University Research Council, Vanderbilt University, which provided travel funds, and to the National Academy of Sciences for its endorsement of Dr. Čársky's visit. We are especially grateful to Drs. J. E. Bertie and M. Torres of the University of Alberta for infrared intensities of the thiirenes and to Ms. Kaara Ettesvold at the Academy for her efforts in our behalf. We also thank Dr. Pêter Pulay for making his program TEXAS available to us.

Appendix

Although the geometry of each molecule studied was optimized only within the restrictions of C_{2v} or C_s symmetry, the vibrational results imply that even if these symmetry restrictions were removed, the reported geometries would remain local energy minima. This is proved by showing that all first derivatives of the potential vanish either by symmetry or by construction; and then, since the force constant matrix is positive definite, all motions increase the potential energy.

Let $x_1, x_2, \ldots, x_{3N-6}$ be symmetry-adapted internal coordinates for the molecule in question, and let $X_i = x_i - x_i^0$ be the displacement of these coordinates from the values x_i^0 in the molecule optimized with symmetry restrictions. Suppose $\mathcal{R}$ is any molecular symmetry operator for the molecule. The potential surface V is unaffected by $\mathcal{R}$

$$\mathcal{R}V(X_1,X_2,\ldots,X_{3N-6}) = V(X_1,\ldots,X_{3N-6}) \qquad \text{(A1)}$$

(A1) needs a little clarification since $\mathcal{R}$ is an operator in the 3-space of the molecule while V is a function in $(3N - 6)$-space. However, each X_i can be represented in 3-space by displacement vectors attached to appropriate atoms of the molecule. Application of $\mathcal{R}$ to the molecule turns each X_i into some combination of the set and hence $\mathcal{R}X_i$ is defined. Thus $\mathcal{R}V$ is to be interpreted as $V(\mathcal{R}X_1,\mathcal{R}X_2,\ldots)$. Any distortion of the molecule from its original position can be represented as a superposition of the X_i. In vibrational problems it is usual to think of $\mathcal{R}$ as operating on these displacement vectors but leaving the atoms unmoved. Equivalently, one could move the atoms and leave the displacement vectors fixed. With this interpretation, the truth of (A1) is clear since $\mathcal{R}$ interchanges only identical atoms and the displaced molecule looks the same before and after the application of $\mathcal{R}$.

Expand V as a series in the X_i and apply $\mathcal{R}$

$$\mathcal{R}V = V_0 + \sum_i \left.\frac{\partial V}{\partial X_i}\right|_0 (\mathcal{R}X_i) + \frac{1}{2}\sum_{i,j}\left.\frac{\partial^2 V}{\partial X_i \partial X_j}\right|_0 (\mathcal{R}X_i)(\mathcal{R}X_j) + \ldots \qquad \text{(A2)}$$

since V_0, $(\partial V/\partial X_i)|_0$, and $(\partial^2 V/\partial X_i \partial X_j)|_0$ are constants. There are no degenerate vibrations in the molecules studied so that

$$\mathcal{R}X_i = \epsilon_i X_i \qquad \text{(A3)}$$

where $\epsilon_i = \pm 1$ for all X_i and for all $\mathcal{R}$ in the appropriate symmetry group. In optimizing the geometry with the symmetry constraints, only totally symmetric X_i (i.e., $\epsilon_i = +1$ for all $\mathcal{R}$) were varied. For these, $(\partial V/\partial X_i)|_0 = 0$ by construction. For the other X_i, there is at least one $\mathcal{R}$ for which $\mathcal{R}X_i = -X_i$. Combining this with (A1) gives

$$\left.\frac{\partial V}{\partial X_i}\right|_0 X_i = \left.\frac{\partial V}{\partial X_i}\right|_0 (-X_i) \qquad \text{(A4)}$$

so that $(\partial V/\partial X_i)|_0 = 0$ by symmetry for the nontotally symmetric motions. Thus all linear terms in the potential vanish, leaving after transforming to normal coordinates

$$V = V_0 + \frac{1}{2}\sum_i \lambda_i Q_i^2 + \ldots \qquad \text{(A5)}$$

The matrix

$$\left[\left.\frac{\partial^2 V}{\partial X_i \partial X_j}\right|_0\right]$$

was obtained by taking numerical derivatives of the $\partial V/\partial X_i$ which were computed analytically. It is found to be positive definite so that all $\lambda_i > 0$. Any molecular distortion and the corresponding potential energy can be expressed either in terms of the symmetry-adapted internal coordinates or the normal modes (eq A5). All the quadratic terms in (A5) are positive. Therefore, all small distortions of the molecule from its optimum symmetry-constrained geometry lead to an increase in energy, and the symmetry-constrained optimum geometry would remain an optimum geometry even if the symmetry constraints were removed.

Registry No. 1, 157-20-0; **2**, 157-18-6; **3**, 157-17-5; thiirene-*d_2*, 65923-97-9; thiirene-*2,3*-$^{13}C_2$, 84057-45-4; thiirene-*d_1*, 63965-75-3; thiirene-*2*-$^{13}C_1$, 63965-74-2; oxirene-*d_2*, 84057-46-5; oxirene-*2,3*-$^{13}C_2$, 84057-47-6; oxirene-*d_1*, 84057-48-7; oxirene-*2*-$^{13}C_1$, 84057-49-8; 1-*H*-azirine-*1*-*d_1*, 84057-50-1; 1-*H*-azirine-*2,3*-*d_2*, 84057-51-2; azirine-*d_3*, 84057-52-3; 1-*H*-azirine-*2,3*-$^{13}C_2$, 84064-67-5; 1-*H*-azirine-*2*-*d_1*, 84057-53-4; 1-*H*-azirine-*1,2*-*d_2*, 84057-54-5; 1-*H*-azirine-*2*-$^{13}C_1$, 84057-55-6.

Location of Cupric Ions in X Zeolites by Electron Spin Echo Spectrometry: Contrast between Sodium and Potassium X Zeolites

Tsuneki Ichikawa[†] **and Larry Kevan***

Contribution from the Faculty of Engineering, Hokkaido University, Sapporo, 060, Japan, and Department of Chemistry, University of Houston, Houston, Texas 77004.

Received April 22, 1982

Abstract: Electron spin echo spectra have been measured for X zeolite containing a small amount of Cu^{2+}. Locations of the Cu^{2+} and the structure of adsorbed molecules have been determined by analyzing the observed nuclear modulation effects on the electron spin echo spectra. In hydrated sodium X zeolite Cu^{2+} is located in hexagonal prisms connecting two sodalite units (site SI), where they are fully coordinated to six lattice oxygens. Upon dehydration at 673 K, the Cu^{2+} environment changes slightly as shown by resolved hyperfine splittings in the $g_\perp$ region and a shorter Cu^{2+}–aluminum distance. Cu^{2+} is still thought to be in site I but may be displaced somewhat toward the sodalite cage. In hydrated potassium X zeolite Cu^{2+} is in sites on a line perpendicular to hexagonal windows between the sodalite and super cages and displaced into the super cages (site SII*). Each Cu^{2+} in site SII* is coordinated to three lattice oxygens in the hexagonal window and three water molecules in the super cage. Upon partial dehydration of the potassium X zeolite at 373 K in air, part of the Cu^{2+} migrate into a site in the center of the hexagonal windows (site II), where each Cu^{2+} is coordinated to three lattice oxygens and two water molecules, one in a sodalite cage and the other in a super cage. In dehydrated potassium X zeolite Cu^{2+} moves to the same site as in dehydrated sodium X zeolite. The difference in the site locations in *hydrated* sodium and potassium X zeolites is explained in terms of the different hydration energies of alkali cations.

Introduction

The cation locations in zeolite catalysts have been extensively studied because of their influence on catalytic properties. When the cations are paramagnetic, electron spin resonance (ESR) spectroscopy has been widely used to gain information about the location and coordination environment of the cations.[1] Cupric ion has been widely studied because this d^9 ion has an easily observed ESR spectrum which is rather sensitive to the Cu^{2+} environment.[2,3] However, the ESR spectrum does not give direct information about the local structure of the cations, such as the distance and number of first solvation shell nuclei. When the cations are surrounded by magnetic nuclei, this information is directly included in the superhyperfine interaction between the electron spins and the nuclear spins, but this is generally too weak for detection by normal ESR.

We have recently demonstrated that electron spin echo (ESE) spectroscopy is useful for selectively detecting the weak superhyperfine interaction between surrounding magnetic nuclei and paramagnetic species on catalytic oxides.[4-12] This superhyperfine interaction shows up as a modulation of the decay of the time domain ESE spectrum. By proper analysis of this modulation one can determine types, number, and distances of magnetic nulcei surrounding the paramagnetic species.[13]

In the present work ESE spectrometry is used to elucidate the local structure of trace Cu^{2+} in hydrated and dehydrated zeolite X with sodium and potassium as exchangeable cations. It is shown that the site location is critically dependent on the nature of the major cation.

Experimental Section

Binder-free Linde 13X (Na–X) was used as a starting material. Potassium X zeolite (K–X) was prepared by conventional exchange of Na^+ in Na–X with K^+. Partially Cu^2 exchanged Na–X and K–X (CuNa–X and CuK–X, respectively) were prepared by ion exchanging as described previously.[4] The extent of exchange of Na^+ or K^+ by Cu^{2+} was approximately 0.3%. After filtration the excess amount of water was taken out by pressing the wet samples between filter paper. The resulting samples are designated as hydrated. Deuterated counterparts of the hydrated samples were prepared by exchanging all the H_2O with D_2O (Stohler Isotope Chemicals) at ambient temperature. Completely dehydrated samples were prepared by evacuating the hydrated samples at ambient temperature for 1 h, heating up to 673 K at increasing temperature for intervals of 1 h in vacuo, oxidizing at 673 K for 2 h under an oxygen pressure of 760 torr, and then evacuating for 15 h at 673 K. Methanol (Merck, spectroscopic grade) and its deuterated counterparts (Stohler Isotope Chemicals) were used as received. These compounds were adsorbed by exposing the dehydrated samples to the vapor at room temperature.

ESR spectra were obtained at 77 K on a Varian E-4 spectrometer. ESE spectra were obtained at 4.2 K on a home-built spectrometer with 1-kW maximum microwave power and typical pulse widths of 20 ns.[14] The nuclear modulations from Al in the zeolite framework were detected by measuring the two-pulse ESE spectra of the zeolite containing no

---

[†] Hokkaido University.

* Author to whom inquiries should be addressed at University of Houston.

(1) Lunsford, J. H. *Adv. Catal.* **1976**, *26*, 137.
(2) Conesa, J. C.; Soria, J. *J. Chem. Soc., Faraday Trans. 1* **1979**, *75*, 406.
(3) Herman, R. G.; Flentge, D. R. *J. Phys. Chem.* **1978**, *82*, 720.
(4) Ichikawa, T.; Kevan, L. *J. Chem. Soc., Faraday Trans. 1* **1981**, *77*, 2567.
(5) Ichikawa, T.; Kevan, L. *J. Am. Chem. Soc.* **1981**, *103*, 5355.
(6) Narayana, M.; Li, A. S. W.; Kevan, L. *J. Phys. Chem.* **1981**, *85*, 132.
(7) Ichikawa, T.; Yoshida, H.; Kevan, L. *J. Chem. Phys.* **1981**, *75*, 2485.
(8) Ichikawa, T.; Yoshida, H.; Kevan, L. *J. Phys. Chem.* **1982**, *86*, 881.
(9) Ichikawa, T.; Kevan, L. *J. Am. Chem. Soc.* **1980**, *102*, 2650.
(10) Narayana, M.; Kevan, L. *J. Am. Chem. Soc.* **1981**, *103*, 5729.
(11) Narayana, M.; Kevan, L. *J. Chem. Phys.* **1981**, *75*, 3269.
(12) Narayana, M.; Kevan, L. *J. Chem. Phys.* **1982**, *76*, 3999.
(13) Kevan, L. In "Time Domain Electron Spin Resonance"; Kevan, L.; Schwartz, R. N.; Eds.; Wiley-Interscience: New York, 1979; Chapter 8.
(14) Ichikawa, T.; Kevan, L.; Narayana, P. A. *J. Phys. Chem.* **1979**, *83*, 3378.

0002-7863/83/1505-0402$01.50/0